Journal for ImmunoTherapy of Cancer

Novel intravesical bacterial immunotherapy induces rejection of BCG-unresponsive established bladder tumors

Eduardo Moreo ,[1,2] Santiago Uranga,[1,2] Ana Picó,[1,2] Ana Belén Gómez,[1,2] Denise Nardelli-Haefliger,[3] Carlos del Fresno ,[4,5] Ingrid Murillo,[6] Eugenia Puentes,[6] Esteban Rodríguez,[6] Mar Vales-Gómez,[7] Julian Pardo ,[2,8] David Sancho ,[5] Carlos Martín ,[1,2] Nacho Aguilo [1,2]

To cite: Moreo E, Uranga S, Picó A, *et al*. Novel intravesical bacterial immunotherapy induces rejection of BCG-unresponsive established bladder tumors. *Journal for ImmunoTherapy of Cancer* 2022;**10**:e004325. doi:10.1136/jitc-2021-004325

► Additional supplemental material is published online only. To view, please visit the journal online (http://dx.doi.org/10.1136/jitc-2021-004325).

Accepted 09 June 2022

For numbered affiliations see end of article.

Correspondence to
Dr Nacho Aguilo;
naguilo@unizar.es

ABSTRACT

Background Intravesical BCG is the gold-standard therapy for non-muscle invasive bladder cancer (NMIBC); however, it still fails in a significant proportion of patients, so improved treatment options are urgently needed.

Methods Here, we compared BCG antitumoral efficacy with another live attenuated mycobacteria, MTBVAC, in an orthotopic mouse model of bladder cancer (BC). We aimed to identify both bacterial and host immunological factors to understand the antitumoral mechanisms behind effective bacterial immunotherapy for BC.

Results We found that the expression of the BCG-absent proteins ESAT6/CFP10 by MTBVAC was determinant in mediating bladder colonization by the bacteria, which correlated with augmented antitumoral efficacy. We further analyzed the mechanism of action of bacterial immunotherapy and found that it critically relied on the adaptive cytotoxic response. MTBVAC enhanced both tumor antigen-specific $CD4^+$ and $CD8^+$ T-cell responses, in a process dependent on stimulation of type 1 conventional dendritic cells. Importantly, improved intravesical bacterial immunotherapy using MBTVAC induced eradication of fully established bladder tumors, both as a monotherapy and specially in combination with the immune checkpoint inhibitor antiprogrammed cell death ligand 1 (anti PD-L1).

Conclusion These results contribute to the understanding of the mechanisms behind successful bacterial immunotherapy against BC and characterize a novel therapeutic approach for BCG-unresponsive NMIBC cases.

WHAT IS ALREADY KNOWN ON THIS TOPIC

⇒ Intravesical BCG is nowadays the gold-standard therapy for high-risk non-muscle invasive bladder cancer (NMIBC), although it fails in a substantial proportion of patients. The therapeutic options for BCG-refractory cases are limited, with radical cystectomy being the most probable outcome. Therefore, there is an urgent need to develop new treatments for high-risk NMIBC, especially for those patients who do not respond to BCG.

WHAT THIS STUDY ADDS

⇒ Here, we demonstrate that MTBVAC, a live attenuated mycobacterial vaccine currently under clinical evaluation for preventing tuberculosis infection, can reject established bladder tumors in a preclinical orthotopic model which is unresponsive to BCG. Intravesical MTBVAC efficacy was further improved by administration of the immune checkpoint inhibitor antiprogrammed cell death ligand 1, and we show that its mechanism of action relied on the stimulation of adaptive immune responses.

HOW THIS STUDY MIGHT AFFECT RESEARCH, PRACTICE, OR POLICY

⇒ Our results provide a solid rationale for further evaluation of intravesical MTBVAC for the treatment of BCG refractory NMIBC.

BACKGROUND

Bladder cancer (BC) is one of the most frequently occurring types of cancer at a global level.[1] Established more than four decades ago, intravesical administration of the mycobacterium BCG is still a first-line therapy for intermediate and high-risk non-muscle-invasive bladder cancer (NMIBC) to prevent progression and recurrence after transurethral tumor resection.[2 3] However, there are a significant number of patients who are resistant to BCG therapy and develop tumor recurrence episodes, especially those ones who must interrupt the treatment due to severe adverse events.[4 5] Currently, there are no established or effective therapies for BCG-unresponsive patients, with radical cystectomy being the standard of care in this setting. In 2020, antiprogrammed cell death 1 (PD-1) checkpoint blockade immunotherapy (pembrolizumab) was approved for BCG-unresponsive NIMBC, although its efficacy remains modest in this setting, with only 20% of all treated patients in remission

at 1 year (Food and Drug Administration (FDA) Advisory Committee Briefing Document 2019 at www.fda.gov/media/133542/download). Apart from this therapy, the only other available option is intravesical administration of valrubicin, which offers only a modest 16% 12-month disease-free rate. Thus, there is an urgent need for developing therapeutic approaches for BCG-unresponsive disease, as well as alternatives to BCG for NMIBC, to avoid extirpation of the bladder, an intervention which is associated with a high incidence of post-operative complications, as well as a significant loss of quality life. Considering its historical success in treating patients with NIMBC, conceivably bacterial immunotherapy could still be improved, either in monotherapy or in combination with immune checkpoint blockade-based treatments.

Despite the long history of BCG as BC immunotherapy, the exact immunological pathways behind its therapeutic efficacy are not completely understood. However, there is a consensus about the need of a competent immune system and the implication of both innate and adaptive arms in the process.[6] Less is known about the bacterial factors behind the antitumoral effect of BCG in BC, although it is believed that a close contact of BCG with the bladder epithelium is needed, in a process shown to involve fibronectin-attachment proteins.[7]

MTBVAC is a live attenuated mycobacterium based on the rational attenuation of a *Mycobacterium tuberculosis* clinical isolate, by deletion of the virulence genes *phoP* and *fadD26*.[8] Intradermal MTBVAC is currently under clinical evaluation as tuberculosis vaccine, demonstrating to be safe and immunogenic both in human newborn and adult populations,[9 10] and it is expected to start efficacy trials as BCG replacement strategy in 2022 (NCT04975178). Our previous data described that intravesical MTBVAC is effective in an experimental mouse model of BC.[11] Even though MTBVAC and BCG present a high degree of genetic homology (>99%), the differences between both strains are mostly defined and have a significant impact in the differential immunogenicity of both vaccines.[12]

In the present study, we conducted a head-to-head comparative study of BCG with MTBVAC, a relevant live attenuated mycobacterium in the context of tuberculosis vaccines, in an orthotopic BC mouse model, to identify whether bacterial genetic differences could influence the antitumoral potential of the bacteria. Our data revealed profound differences between both vaccines, showing an improved capacity of MTBVAC to potentiate $CD4^+$ and $CD8^+$ T-cell tumor-specific responses, which induced rejection of bladder tumors in a setting in which BCG did not confer any survival advantage compared with untreated controls. Importantly, we found that the presence of BCG-absent genes *esat6* and *cfp10* in MTBVAC results is crucial for the bacteria to colonize more efficiently the bladder following intravesical instillation, and to induce an efficient therapeutic response.

METHODS

Mouse strains

All mice were housed and maintained in specific pathogen-free conditions and observed for any sign of disease. Female C57BL/6JR mice 8–10 weeks old were purchased from Janvier Biolabs. Mouse strains deficient in Rag1 ($Rag1^{KO}$) and interferon gamma (IFN-γ^{KO}) bred on the B6 background were purchased from Jackson Laboratories. The mouse strains deficient in perforin ($Perf^{KO}$) and Batf3 ($Batf3^{KO}$) were bred in the CIBA animal facilities.

Cell lines

MB49 BC cells and B16F10 melanoma cells were purchased from the American Type Culture Collection (ATCC). MB49-cells expressing green-fluorescence protein (GFP) were provided by Denise Nardelli-Haefliger.[13] MB49-ZsGreen-Luc cells were constructed in the laboratory by transfection with a lentivirus encoding ZsGreen and firefly luciferase. For the generation of MB49-$B2m^{KO}$ cells, parental MB49 cells were transfected with plasmids targeting the *B2m* gene (Santa Cruz Biotechnology) and cells were selected with puromycin and then sorted based on lack of major histocompatibility complex type I (MHC-I) expression after staining with an antibody directed to $H2K^b/D^b$ (Miltenyi Biotech). Cells were cultured with complete Dulbecco's Modified Eagle Medium (DMEM), containing 10% inactivated fetal bovine serum (FBS), Glutamax (Sigma) and penicillin/streptomycin (Sigma) and were always used with less than 10 passages from thawing.

Bacterial strains

Mycobacterial strains used in this study were grown at 37°C in Middlebrook 7H9 broth (BD Difco) supplemented with 0.05% Tween 80 (Sigma) and 10% Middlebrook albumin dextrose catalase enrichment (ADC, BD Biosciences) or on solid Middlebrook 7H10 agar (BD Difco) supplemented with 10% ADC (BD Biosciences).

BCG Tice was obtained and cultured from a commercial vial of OncoTICE. BCG Pasteur 1173P2 and BCG::RD1 were a kind gift from Roland Brosch (Institut Pasteur, France). GFP-expressing MTBVAC and BCG Tice strains were generated in the laboratory by transformation with the pJKD6 plasmid (a kind gift from Luciana Leite, Butantan Institute, Brazil). The MTBVAC strain lacking ESAT6 and CFP10 (MTBVAC ΔE6C10) was constructed and characterized in our laboratory.[12]

Orthotopic implantation of MB49 cells

For the MB49 orthotopic BC model, female mice 8–10 weeks old were anesthetized with isoflurane and intravesically instilled with 50 µL of a 0.01% poly-L-lysine (Sigma) solution using a 24-gage catheter (BD Insyte) attached to a syringe. The poly-L-lysine solution was maintained in the bladder for 20 min, and then the catheter was removed and the bladder was emptied by manually applying gentle pressure. Then 50 µL of a solution containing

4×10^5 MB49 cells was intravesically instilled and retained in the bladder for 1 hour, after which the bladder was emptied and the mice were allowed to recover from anesthesia. The mice were observed and weighted every 2 days and scored based on weight loss, presence of haematuria, visible signs of growing tumor, and general behavior, and were euthanized when reaching the predefined and approved endpoint criteria.

Intravesical bacterial treatments

Mice were anesthetized and intravesically instilled using a 24-gage catheter with 50 µL of a solution containing 5×10^6 bacteria diluted in phosphate buffered saline (PBS) and maintained in the bladder for 2 hours. Then the bladder was manually emptied and the mice were allowed to recover from anesthesia.

Subcutaneous and intravenous tumor challenges

MB49 or B16F10 cells resuspended in serum-free DMEM were injected subcutaneously in the flank of mice (5×10^5 cells) or intravenously (7×10^5 cells). The size of subcutaneous tumors was measured with a caliper and determined by using the following formula: [(tumor width)^2×(tumor length)]/2. Mice were sacrificed when tumor volume exceeded 1 cm^3.

Antibody-based cell depletion and treatments

For CD4 and CD8 depletion, mice were injected intraperitoneally with 300 µg of anti-CD4 (clone GK1.5, BioXCell) or 300 µg of anti-CD8α (clone 2.43, BioXCell) 3 days before tumor challenge or the day before intravesical treatment. Repeated doses were administered to achieve continuous depletion if needed. For antibody-based treatment, 200 µg of αPD-L1 (clone 10F.9G2, BioXCell) was injected intraperitoneally two times a week.

Bacterial load determination in tissues

Bladders and bladder draining lymph nodes (dLNs) were harvested and homogenized using a GentleMacs dissociator (Miltenyi). Serial dilutions were prepared in PBS, plated in solid 7H10 medium supplemented with 10% ADC, and 3 weeks later colony-forming units (CFUs) were counted.

Preparation of single-cell suspensions

Bladder cell suspensions were prepared by manual dissociation using scissors and a scalpel, followed by digestion in Roswell Park Memorial Institute (RPMI) medium containing 0.17 U/mL Liberase (Roche), 2 mg/mL Collagenase D (Roche) and 40 U/mL DNAse I (ApplyChem) for 45 min at 37°C, followed by filtration through a 70 µM cell strainer (MACS SmartStainers, Miltenyi Biotec). Red blood cells (RBCs) were lysed in 1 mL RBC lysing buffer (Sigma-Aldrich) for 1 min. Spleens and lymph nodes were mashed with the back of a syringe in RPMI with 2 mg/mL Collagenase D and 40 U/mL Dnase I, incubated for 20 min at 37°C and strained through a 70 µM cell strainer before lysing erythrocytes with RBC lysing buffer for 1 min. Single cells were resuspended in PBS with 2% FBS and stained for surface and intracellular markers.

Flow cytometry

Single cells were incubated with mouse Fc receptor blocking reagent (Miltenyi) for 20 min at 4°C, washed, and stained with fluorochrome-conjugated antibodies for 20 min at 4°C. Cells were acquired using a Gallios flow cytometer (Beckman Coulter).

The following antibodies were used (from Miltenyi unless otherwise noted): CD45-Vioblue, clone REA737; CD45-PerCP-Vio770, clone REA737; CD11b-PerCP-Vio700, clone REA592; CD11c-PerCP-Vio700, clone REA754; CD11c-PE, clone REA754; F4/80-PE, clone REA126; XCR1-APC, clone REA707; MHCII-Vioblue, clone REA813; H2K^b/D^b-APC, clone REA932; CD3-PerCP-Vio700, clone REA641; CD4-FITC, clone REA604; CD8-PE, clone REA 601; CD8-APC, clone REA601; PD1-APC, clone J43 (BD); CD86-VioBright, clone REA1190; CD86-PE, clone REA1190; CD172α-APC-Vio-770 (Sirpα), clone REA1201; CD223-FITC (LAG-3), clone C9B7W; NKp46-PE, clone REA815, PD-L1-PE, clone MIH5 (BD).

Restimulation and intracellular cytokine staining

Single-cell suspensions were stimulated with phorbol-12-myristate 13-acetate (PMA) (50 ng/mL, Sigma-Aldrich) and ionomycin (1 µg/mL, Sigma-Aldrich) in the presence of brefeldin A (eBioscience) for 4 hours at 37°C before cell surface and intracellular staining with FoxP3 staining set (Miltenyi). After fixation and permeabilization, the following antibodies from Miltenyi were used: IFN-γ-APC, clone REA638.

IFN-γ ELISPOT

Splenocytes (5×10^5) were seeded in 96-well ELISPOT plates (MSIP PVDF-plates, Millipore) precoated with primary anti-mouse IFN-γ antibody (Mouse IFN-γ ELISpot^{BASIC} kit HRP, Mabtech) and incubated overnight with either only media or 10 µg/mL of Dby HY I-*Ab* restricted peptide (NAGFNSNRANSSRSS) or the H-2D^b Uty HY peptide (WMHHNMDLI). The next day, IFN-γ-producing colonies were detected using a biotinylated anti-mouse IFN-γ detection antibody. Spot-forming units were automatically counted using AID Elispot Reader (GmbH).

Cytotoxicity assay

MB49-ZsGreen-Luc cells were seeded in 96 well-plates as target cells. Splenocytes from MB49 tumor-bearing animals were isolated as described and seeded at a 100:1 ratio over the target cells for 24 hours. Then, 150 µg/mL of Xenolight D-luciferin Potassium Salt (PerkinElmer) was added to the wells, incubated for 15 min at 37°C, and luminescence was measured in an Epoch Microplate reader (BioTek). Percent cytotoxicity was calculated with reference to the cytotoxicity exerted by splenocytes isolated from a naïve non-tumor-bearing animal using the following formula: [100–(experimental luminescence/naïve luminescence)×100].

Data analysis

Tumor-bearing mice were randomized into different treatment groups. To avoid cage-associated variability, each cage contained mice from every experimental groups. The number of biological replicates and repetitions for each experiment is indicated in figure legends. Animal monitoring and data analysis were not blinded. Flow cytometry data were analyzed using Weasel software V.3.0.2 following gating strategies shown in online supplemental figure S1. GraphPad Prism software V.8 was used for graphical representation and statistical analysis. Data were analyzed using the Grubb's test for statistical outliers using an α value of 0.01. All tests applied were two-sided. The group means for different treatments were compared by analysis of variance with Bonferroni's multiple comparisons test, or by a two-sided Student t-test. Survival was analyzed by the log-rank (Mantel-Cox) test. P values of <0.05 were considered significant.

RESULTS

Bacterial bladder colonization correlates with better antitumoral efficacy

BCG attachment and internalization within the bladder epithelium have been reported to be crucial for bacterial antitumoral effect in animal models.[7 14] First, we wanted to assess whether bacterial bladder colonization ability was distinctive in each of the strains tested. We compared BCG and MTBVAC in a well-accepted orthotopic BC model, based on the instillation of syngeneic murine MB49 bladder tumor cells. Tumor-bearing mice were treated with BCG Tice or MTBVAC as indicated in figure 1A, and bladders and the corresponding dLNs were harvested to determine bacterial load. We found a higher amount of viable MTBVAC bacilli both in bladder (figure 1B) and dLNs (figure 1C) compared with BCG.

We then studied whether BCG and MTBVAC were differentially internalized by bladder cells. To assess this, we treated MB49 tumor-bearing mice with GFP-tagged vaccines, and 2 hours after the second instillation, we analyzed GFP^+-infected cells by flow cytometry (figure 1D,E). The percentage of GFP^+ cells was significantly higher in the case of MTBVAC compared with BCG (figure 1F), confirming the results obtained by bacterial load determination. In addition, around 95% of the infected cells were found $CD45^+$, both in the case of BCG and MTBVAC (figure 1G), demonstrating that under in vivo conditions, bacterial internalization is mainly restricted to immune cells. Altogether, these results revealed that different live attenuated mycobacteria present disparate ability to colonize the bladder following intravesical instillation.

Then we tested whether bacterial bladder colonization correlated with antitumoral efficacy, evaluating survival progression in the different experimental groups. In agreement with previous studies, we found that in this model, the length of the interval between tumor cell challenge and the first BCG instillation is highly determinant for vaccine antitumoral efficacy.[11 15–17] When BCG instillation regime started the day after tumor engraftment, bacteria provided better protection compared with PBS-treated mice (figure 1H), whereas treatment efficacy was abrogated when the first vaccine instillation was performed 3 days after tumor challenge (figure 1I). To assess whether intravesical BCG immunotherapy could be improved by MTBVAC, we compared them initiating the treatment regime 3 days after tumor challenge, under conditions that could mimic BCG-unresponsive tumors. Under these settings, intravesical MTBVAC immunotherapy provided a strong protection against MB49 tumors, with 75% of the mice surviving at the end of the 70-day follow-up, compared with 22% in the case of BCG (figure 1I). These results indicated that bacterial bladder colonization might be a key factor behind antitumoral efficacy.

esat6 and *cfp10* genes absent in BCG are crucial for improved bladder colonization and antitumoral efficacy

Next, we wanted to explore the genetic differences between BCG and MTBVAC that could explain their distinctive bladder colonization ability. MTBVAC conserves the genes *esat6* and *cfp10*, which are contained in the RD1 genomic region absent in BCG,[18] and whose absence represents the main cause of attenuation for BCG.[19] ESAT6 and CFP10 proteins have been described to participate in bacterial attachment to the lung epithelium.[20] Thus, to test a possible contribution of these proteins to bacterial bladder colonization, we made use of an *esat6/cfp10* double mutant MTBVAC strain (MTBVAC ΔE6C10), previously generated and characterized in our laboratory.[12] The enhanced capacity of MTBVAC over BCG to colonize the bladder and migrate to dLNs on intravesical instillation was abolished in the ΔE6C10 mutant, both in tumor-bearing (figure 2A,B) and tumor-free mice (figure 2C,D). Interestingly, an RD1-complemented BCG strain, which expresses ESAT6 and CFP10, recovered the ability of the bacteria to colonize the bladder (figure 2E), strongly suggesting an important contribution of these proteins in mediating bacterial bladder internalization. The lower colonization and dLN dissemination observed with BCG and the MTBVAC ΔE6C10 strain concurred with a lower infiltration of total $CD45^+$ leukocytes (figure 2F) and $CD4^+$ and $CD8^+$ T lymphocytes (figure 2G) into the bladders of mice compared with the MTBVAC-treated group. We also found a significant correlation between the number of viable bacilli found in the dLN from the different animals instilled with bacteria and the number of bladder-infiltrating $CD4^+$ and $CD8^+$ T lymphocytes (figure 2H), suggesting a direct connection between the efficacy of the bacteria to colonize the bladder and the local inflammatory response.

Finally, MTBVAC ΔE6C10 therapeutic efficacy in the MB49 model was substantially reduced to levels comparable to those observed with BCG, and only 9% of the mice survived at the end of the follow-up (figure 2I). Thus, our results indicated that the differential expression of

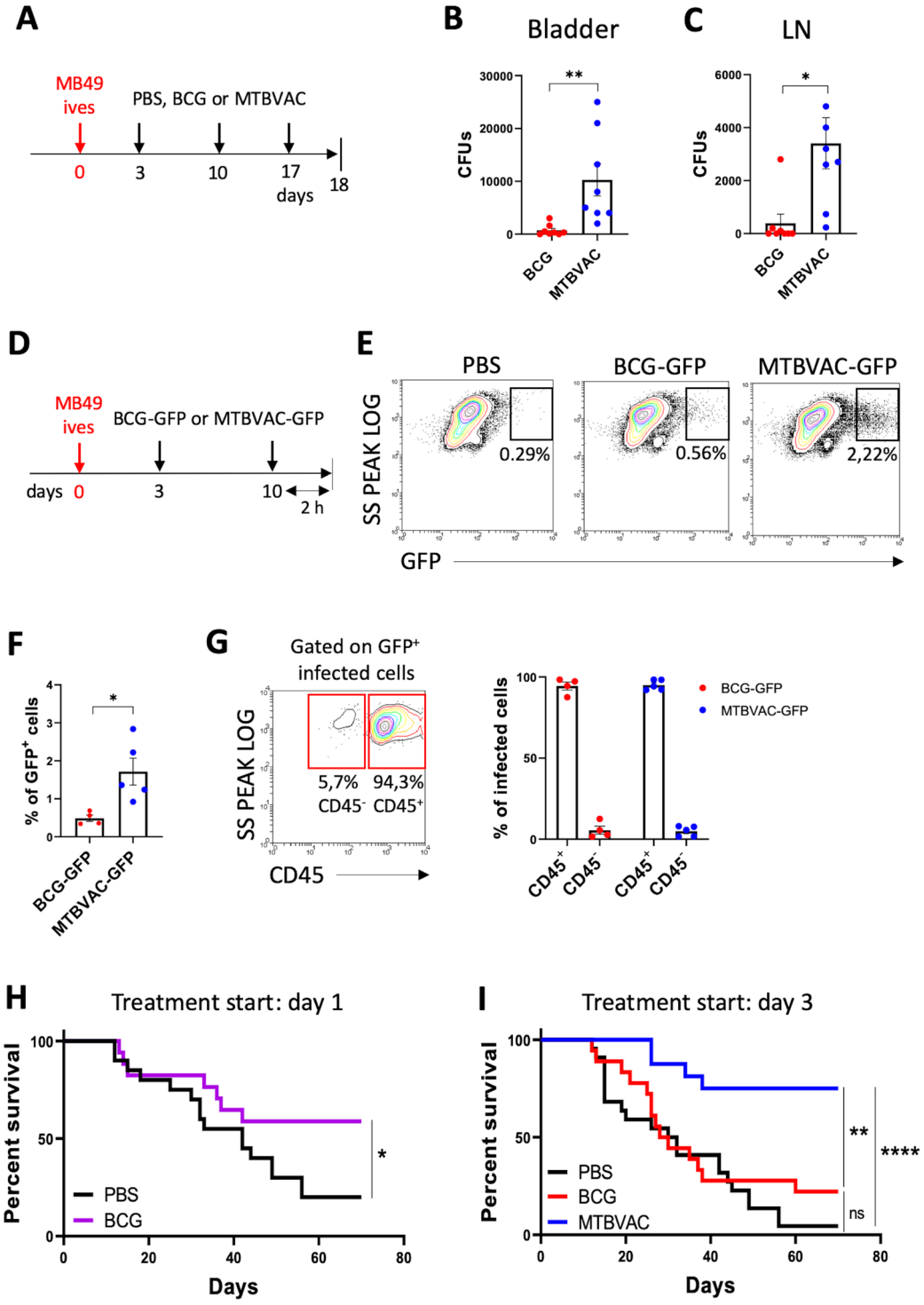

Figure 1 Superior efficacy of MTBVAC against bladder cancer correlates with better colonization capacity. (A) Schedule of intravesical treatments of mice bearing orthotopic MB49 bladder tumors with PBS, BCG Tice or MTBVAC. (B,C) Mice were treated as in (A), and at day 18, bladder tumors and draining LNs were extracted and homogenized and total CFUs were enumerated (n=8 mice per group, pooled from two independent experiments). (D) Mice were treated as in (A) with GFP-expressing bacteria and euthanized 2 hours after the second instillation, at day 10. Bladder tumors were extracted; single-cell suspensions were generated; and infected GFP$^+$ cells were identified by flow cytometry. (E) Representative density plots of GFP$^+$ cells. (F) Percentage of GFP$^+$ infected cells (n=4–5 mice per group, pooled from two independent experiments). (G) Representative density plots and distribution of GFP$^+$ infected cells in CD45$^-$ and CD45$^+$ subsets in bladder tumors. (H) Survival of mice bearing MB49 bladder tumors treated with intravesical PBS or BCG at days 1, 8 and 15 post tumor implantation (n=20 PBS, n=18 BCG, pooled from two independent experiments). (I) Survival of mice bearing MB49 bladder tumors treated as in (A) (n=22 PBS, n=18 BCG, n=16 MTBVAC, pooled from two independent experiments). Graphs represent mean±SEM. *P<0.05, **P<0.01, ****P<0.0001, unpaired t-test (B,C,F), or log-rank test (H,I). CFU, colony-forming unit; LN, lymph node.

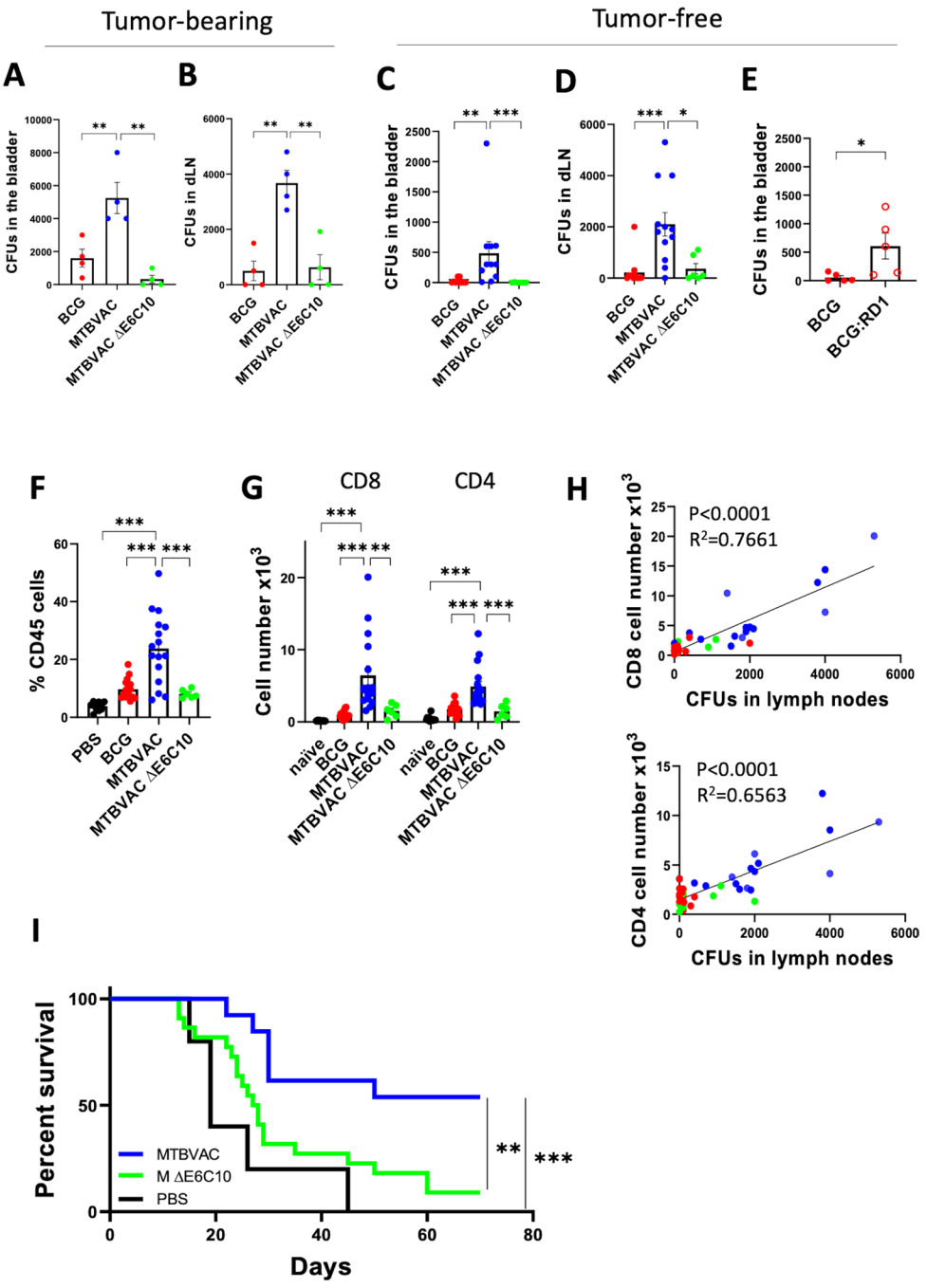

Figure 2 ESAT6 and CFP10 expression on MTBVAC determines improved antitumoral efficacy. (A,B) Tumor-bearing mice were treated with intravesical BCG TICE, MTBVAC or MTBVACΔE6C10 at days 3, 10, and 17, and at day 18, bladders and dLN were extracted and homogenized, and total CFUs were enumerated (n=4 mice per group, from one experiment). (C) Tumor-free mice were intravesically instilled with the indicated bacteria, and 24 hours later bladders were extracted and total CFUs were enumerated (n=6 mice MTBVACΔE6C10 group, n=12 BCG and MTBVAC groups, pooled from two independent experiments). (D) Tumor-free mice were intravesically instilled at days 0, 7, and 14, and at day 15, dLNs were extracted and total CFUs were enumerated (n=6 mice MTBVACΔE6C10 group, n=12 BCG and MTBVAC groups, pooled from two independent experiments). (E) Mice were treated as in (C) with intravesical BCG Pasteur or RD1-recomplemented BCG Pasteur, and total CFUs were enumerated in the bladder 24 hours later (n=5 mice per group, from one experiment). (F–H) Mice were treated as in (D), and at day 15, bladders were extracted; single-ell suspensions were generated; and CD45$^+$, CD4$^+$, and CD8$^+$ cells were identified by flow cytometry (n=6 mice MTBVACΔE6C10 group, n=16 BCG and MTBVAC groups, n=10 PBS group, pooled from three independent experiments). (H) Correlation between CD4$^+$ and CD8$^+$ T cells infiltrated in the bladder and bacterial CFUs in the draining LN, analyzed by linear regression. (I) Survival curve of mice implanted with orthotopic MB49 bladder tumors and treated intravesically with PBS, MTBVAC or MTBVACΔE6C10 at days 3, 10, and 17 (n=5 PBS, n=13 MTBVAC, n=22 MTBVACΔE6C10, pooled from two independent experiments). Graphs represent mean±SEM. *P<0.05, **P<0.01, ***P<0.001, one-way analysis of variance with Bonferroni post-test (A–D,F,G), unpaired t-test (E), or log-rank test (I). CFU, colony-forming unit; dLN, draining lymph node; LN, lymph node.

ESAT6/CFP10 by MTBVAC might explain the improved antitumoral efficacy of this strain compared with BCG.

Adaptive immune system drives MTBVAC antitumoral effect

We next aimed to study the immune pathways involved in MTBVAC-driven antitumoral response. First, we assessed MTBVAC immunotherapy efficacy in Rag1^{KO} mice (figure 3A), which lack T and B cells. Vaccine efficacy was abrogated in these mice, suggesting a critical contribution of the adaptive immune system. However, we observed a minimal survival advantage in the treated group, which suggested a small contribution of innate immune cells. Further confirming a key role of the cytotoxic cellular immune response for therapeutic efficacy, we found that mice lacking perforin (Perf^{KO}) or interferon gamma (IFN-γ^{KO}) treated with bacterial immunotherapy did not survive more than PBS controls (figure 3B,C), indicating that these two molecules are needed for MTBVAC-induced tumor rejection.

These results suggested a crucial role of cytotoxic T cells (CTLs) for MTBVAC therapeutic efficacy. To confirm this finding, we used a variant of the MB49 cells in which we previously disrupted the *B2m* gene using CRISPR-Cas9, which abolished MHC-I cell surface expression (online supplemental figure S2), and therefore were unrecognizable by CTLs. MTBVAC immunotherapy extended survival of mice bearing MB49-*B2m*^{KO} bladder tumors (figure 3D), but to a much lesser extent than on MB49-WT tumors, since no treated mice survived until day 20, a time point in which all MTBVAC treated MB49-WT tumor-bearing mice were still alive (figures 1I and 2E).

To assess whether bacterial treatment could be favoring tumor cell recognition by CTLs, we analyzed MHC-I surface expression over GFP-expressing MB49 cells following vaccine instillation (figure 3E,F). At day 12 post tumor cell inoculation, tumor weights in the MTBVAC group were significantly reduced compared with controls (figure 3G), confirming an early vaccine antitumoral effect. At this time point, bacterial immunotherapy upregulated MHC-I expression on tumor cells compared with controls (figure 3H). This effect was abrogated in IFN-γ^{KO} mice (figure 3H), showing that MHC-I upregulation was not due to a direct interaction of the bacteria with tumor cells, but to an indirect mechanism mediated by immune cell-derived IFN-γ. Our data revealed that CD4$^+$ and CD8$^+$ T cells, both well-known IFN-γ-producing cells, were needed for MHC-I upregulation on tumor cells after bacterial immunotherapy, with CD4$^+$ T cells appearing as the most important subset (figure 3I). Altogether, these results reflect that bacterial immunotherapy induces MHC-I upregulation on the tumor cell surface in an IFN-γ- dependent manner, an event that might be crucial to enhance tumor cell recognition by CTLs.

Improved bacterial immunotherapy boosts T cell-mediated antigen-specific immunity

Although the implication of T cells in the BCG antitumoral mechanism has been described, it is not clear whether BCG induces tumor-specific immunity, or its efficacy is a collateral effect of the vaccine-specific response.[15 16] Trying to address this question, we studied the tumor-specific responses to endogenous antigens. We took advantage of the fact that MB49 cells are of male origin and express antigens contained in the HY chromosome, which are immune reactive when implanted on female hosts.[21] Importantly, T-cell epitopes for the H-2^k haplotype derived from the HY chromosome have been described, and CD4$^+$ and CD8$^+$ T cells specific for these epitopes recognize and eliminate MB49 cells in vitro.[22] Therefore, we induced MB49 bladder tumors and the systemic immune response against the HY-derived peptides Dby and Uty (CD4- and CD8- restricted, respectively) was measured in the spleen at day 12, after two vaccine instillations. Measured by ELISPOT assay, MTBVAC immunotherapy triggered a higher proportion of Dby and Uty-specific IFN-γ-secreting cells compared with BCG and untreated groups (figure 4A).

To confirm the functionality of this tumor-specific response, we showed first that splenocytes derived from MTBVAC-treated mice were more cytotoxic against MB49 cells in vitro than those from untreated mice (figure 4B). This cytotoxicity was abolished in the absence of CD8$^+$ T cells (figure 4B), demonstrating that tumor-specific CTLs were responsible for this effect. Then, we rechallenged MTBVAC-treated survivor mice (which had previously eliminated bladder tumors) with MB49 cells by the subcutaneous route to evaluate the capacity of the preestablished specific response to reject distal tumors. No MB49 tumor growth was observed in any of the animals previously treated with MTBVAC, in comparison to control naïve mice (figure 4C). Depletion of CD4$^+$ and CD8$^+$ T cells (online supplemental figure 3A,B) reverted resistance of survivor mice against rechallenge (figure 4C), confirming the critical role of these cells in driving long-term tumor-specific immune memory. As an additional control, we inoculated another cohort of MTBVAC-treated survivors with non-antigenically related B16F10 melanoma cells in the contralateral flank. Unlike MB49, B16F10 cells induced tumors both in naïve and MTBVAC-treated survivor mice (figure 4D), demonstrating that MB49 tumor rejection relied on a tumor-specific immune memory response. It has been reported that intravenous MB49 cell inoculation generates lung metastasis,.[23] Thus, we also found that MTBVAC-treated surviving mice rejected the intravenous MB49 rechallenge (figure 4E), showing that immune memory generated by bacterial immunotherapy was also effective against disseminated disease.

We then depleted separately CD8$^+$ or CD4$^+$ T lymphocytes (online supplemental figure 3C–E) in MTBVAC-treated mice to study the particular contribution of these cells to bacterial immunotherapy. Bladder weights were significantly higher in CD8$^+$ and CD4$^+$ cell-depleted mice compared with controls (figure 4F), underscoring the importance of adaptive immunity for MTBVAC therapeutic effect. Vaccine-induced CD8$^+$ T-cell infiltration

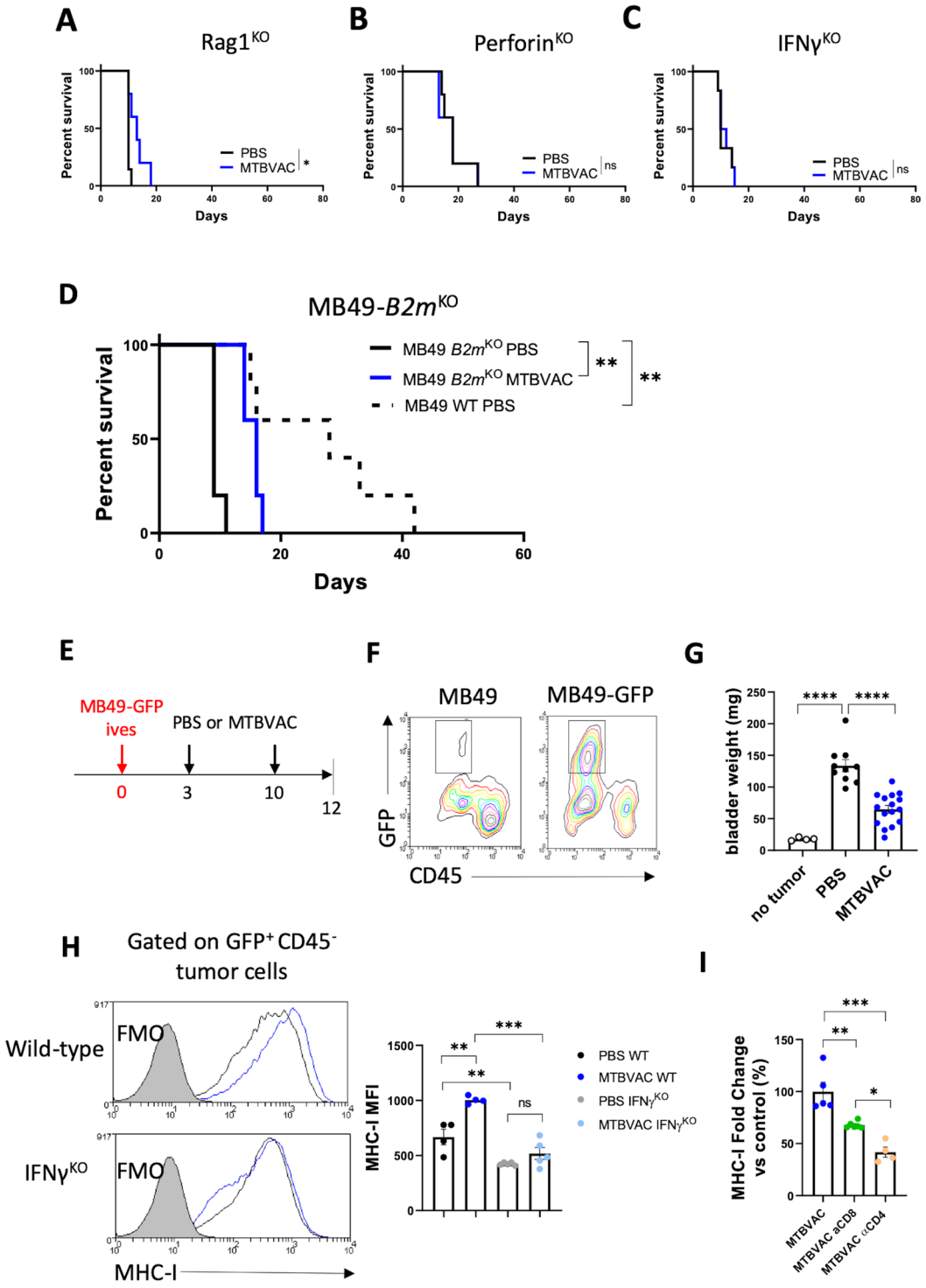

Figure 3 MTBVAC efficacy relies on the adaptive immune system. (A–C) survival curves of Rag1^{KO} (A), Perf^{KO} (B) and IFN-γ^{KO} (C) mice implanted orthotopically with MB49 tumors and treated with either PBS or MTBVAC at days 3, 10, and 17 (n=5–6 mice per group, from one experiment). (D) Survival of mice implanted orthotopically with MB49-*B2m*^{KO} or MB49-WT cells and treated with either PBS or MTBVAC at days 3, 10, and 17 (n=5 mice per group, from one experiment). (E–I) bladder tumors were induced by intravesical instillation of GFP-expressing MB49 cells and mice were treated with either PBS or MTBVAC at days 3 and 10 and euthanized at day 12. (F) Representative density plots of single-cell suspensions from the MB49 and MB49-GFP tumor-bearing bladders. (G) Bladder weights of mice treated as in (E) (n=4 no tumor, n=9 PBS, n=16 MTBVAC, from three independent experiments). (H) Flow cytometry analysis of MHC-I expression on GFP^{+} CD45^{-} tumor cells in vivo (n=4–5 mice per group, representative of two independent experiments). (I) Mice were treated as in (E) but were given αCD4 or αCD8 depleting antibodies the day before intravesical treatments (on days 2 and 9). The graph shows tumor cell MHC-I expression fold change versus the control MTBVAC group (n=4–6 mice per group, pooled from two independent experiments). Graphs represent mean±SEM. *P<0.05, **P<0.01, ***P<0.001, ****P<0.0001 one-way analysis of variance with Bonferroni post-test (G–I) or log-rank test (A–D). FMO, fluorescence minus one; IFN-γ, interferon gamma; ns, not significant; WT, wild type.

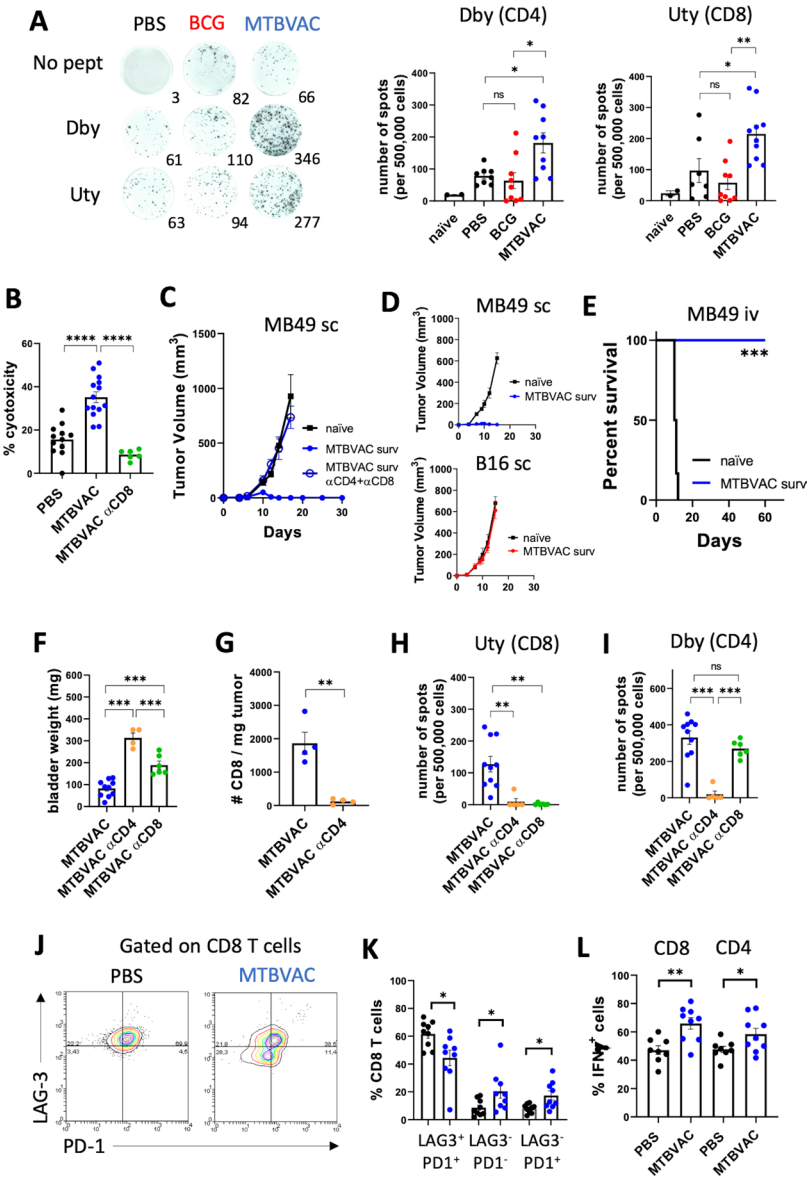

Figure 4 Intravesical MTBVAC augments CD4$^+$ and CD8$^+$ T-cell tumor antigen-specific immunity. MB49 bladder tumors were implanted orthotopically and mice were treated with PBS, BCG or MTBVAC at days 3 and 10. (A) At day 12 post tumor implantation, IFN-γ- producing splenocytes were assessed by ELISPOT following stimulation with 10 µg/mL of the Dby or Uty peptides. Numbers below the representative images indicate the numbers of spots (n=8–9 mice per group, pooled from two independent experiments). (B) In vitro cytotoxic activity of splenocytes against MB49 cells (n=12 mice PBS, n=14 MTBVAC, n=6 MTBVAC αCD8, pooled from three independent experiments). (C) MTBVAC-treated survivors were subcutaneously rechallenged with MB49 cells in the flank, and tumor growth was measured over time. One group of surviving mice was given CD4 and CD8 depleting antibodies 3 days before the rechallenge and 3 days after. Naïve mice were used as controls (n=8–10 mice per group, from two independent experiments). (D) Mice were subcutaneously rechallenged with MB49 cells in one flank and B16F10 in the contralateral flank, and tumor growth was measured over time. Naïve mice were used as controls (n=5–6 mice per group, from one experiment). (E) MTBVAC-treated surviving mice were intravenously rechallenged with MB49 cells. Naïve mice were used as controls (n=6–7 mice per group, from one experiment). (F–I) MB49 tumor-bearing mice treated with MTBVAC were given CD4 or CD8 depleting antibodies and euthanized at day 12. (F) Bladder weights at day 12 post tumor cell inoculation (n=10 mice MTBVAC, n=4 MTBVAC+αCD4, n=6 MTBVAC+αCD8, pooled from two independent experiments). (G) Number of tumor-infiltrating CD8$^+$ T cells per milligram of tumor, identified by flow cytometry in bladder single cell suspensions (n=4 mice per group, one experiment). (H,I) IFN-γ -producing splenocytes after stimulation with the Uty (H) or Dby (I) peptides measured by ELISPOT assay (n=10 mice MTBVAC, n=4 MTBVAC+αCD4, n=6 MTBVAC+αCD8, pooled from two independent experiments). (J–L) Tumor-infiltrating T cells were analyzed by flow cytometry at day 12 in PBS or MTBVAC-treated mice (n=8–9 mice per group, pooled from two independent experiments). (J) Representative density plots of PD-1 and LAG-3 expression by CD8$^+$ T cells. (K) Quantification of CD8$^+$ cells expressing PD-1 and LAG-3. (L) Quantification of tumor-infiltrating CD4$^+$ and CD8$^+$ T cells expressing IFN-γ after ex vivo restimulation with PMA/ionomycin. Graphs represent mean±SEM. *P<0.05, **P<0.01, ***P<0.001, one-way analysis of variance with Bonferroni post-test (A,B,F,H,I) or unpaired T test (G,K,L). IFN-γ, interferon gamma; ns, not significant; PD-1, programmed cell death 1; PMA, phorbol-12-myristate 13-acetate.

in the bladder (figure 4G), as well as the Uty-specific response (figure 4H), was abrogated in the absence of $CD4^+$ T lymphocytes. Dby-specific CD4 response was still present in CD8 depleted mice (figure 4I), which indicates that the initiation of tumor-specific CD4 responses is independent of $CD8^+$ T cells. Collectively, these results suggest that MTBVAC bacterial therapy potentiates a tumor-specific CD4 response that is necessary for the generation of tumor-specific $CD8^+$ T cells and their infiltration into MB49 bladder tumors.

We also assessed whether MTBVAC treatment triggered phenotypical alterations in tumor-infiltrating $CD8^+$ T lymphocytes. After two intravesical treatments, a significant reduction in the proportion of $CD8^+$ T cells expressing PD-1 and LAG-3 was observed in the MTBVAC group (figure 4J,K), a phenotype associated with T-cell exhaustion.[24] Concomitantly, a higher proportion of tumor-infiltrating $CD8^+$ and $CD4^+$ T cells expressed the effector cytokine IFN-γ on PMA/ionomycin restimulation in MTBVAC-treated mice (figure 4L), demonstrating improved functionality of these cells induced by intravesical therapy.

Intravesical bacterial immunotherapy relies on type 1 conventional dendritic cells (cDC1s)

cDC1s are responsible for the processing and cross presentation of tumor antigens and are crucial for the generation of tumor-specific $CD4^+$ and $CD8^+$ T cells.[25] Here we assessed the contribution of cDC1s to MTBVAC-induced tumor-specific response and therapeutic efficacy. First, we identified cDC1s in the bladder 12 days after tumor cell inoculation (figure 5A). As expected, $XCR1^+$ $SIRP\alpha^-$ cDC1s were selectively absent in bladders from $Batf3^{KO}$ mice, which have been described to lack this cell population.[26] Intravesical MTBVAC induced the recruitment of $XCR1^+$ cDC1s to the bladder (figure 5A), and cDC1s of treated mice expressed higher levels of the costimulatory molecule CD86 both in the tumor and in the dLNs (figure 5B). Next, we inoculated mice intravesically with ZsGreen-expressing MB49 cells, which allowed us to track immune cells that had engulfed tumor-associated material (figure 5C). We focused on tumor-draining LNs, where antigen presentation to $CD4^+$ and $CD8^+$ T cells occurs, and found that ZsGreen positivity was mostly restricted to the cDC1 compartment (figure 5D). Our results indicated a higher percentage of $ZsGreen^+$ cells in cDC1s, and not in other cellular compartments, from mice receiving intravesical MTBVAC (figure 5D). Altogether these findings suggested that intravesical MTBVAC is favoring the migration of tumor-antigen loaded and activated cDC1s from the tumor to the LNs, which could explain the enhanced tumor-specific response observed in these mice.

To confirm the functional role of cDC1s in driving the therapeutic response to MTBVAC, we evaluated the survival of $Batf3^{KO}$ mice bearing MB49 bladder tumors. MTBVAC therapeutic efficacy was abrogated in $Batf3^{KO}$ mice (figure 5E), and these animals presented significantly higher bladder weights at day 12 after tumor cell inoculation compared with MTBVAC-treated wild-type mice (figure 5F). Furthermore, $CD8^+$ T-cell infiltration into the bladder was completely abolished in the absence of cDC1s (figure 5G), and concurrently, $Batf3^{KO}$ mice were unable to mount both CD4 and CD8 tumor-specific responses on MTBVAC treatment (figure 5H), as well as to upregulate MHC-I on tumor cell surface (figure 5I).

Rejection of established bladder tumors by bacterial immunotherapy

We finally explored the ability of MTBVAC to eliminate fully established bladder tumors. For this, we chose to start MTBVAC intravesical treatment at day 6 post tumor cell engraftment, since at this timepoint haematuria, one of the first signs of BC detected by patients, started to be apparent. We confirmed that at this timepoint tumors were visible macroscopically on necropsy, and undoubtedly established as demonstrated by histological analysis (figure 6A). In addition, we assayed the combination of intravesical BCG or MTBVAC with antiprogrammed cell death ligand 1 (PD-L1) targeting antibodies since immunotherapy against PD-1/PD-L1 axis has been proven successful in the clinic to treat BCG-unresponsive NMIBC, as well as metastatic muscle-invasive bladder tumors. Supporting this combination, we found an IFN-γ-dependent upregulation of PD-L1 expression on $CD45^+$ SSC^{hi} immune cells following intravesical MTBVAC therapy (figure 6B). We administered six instillations delivered 1 week apart (figure 6C), mirroring the induction phase regime used with BCG in the clinic. Our data revealed that intravesical MTBVAC given as monotherapy was successful in inducing tumor regression in this treatment setting, with 9 out of 15 mice found tumor-free by macroscopic visualization at day 70, confirming the capacity of MTBVAC to induce eradication of established tumors (figure 6D). Strikingly, combination of intravesical MTBVAC with systemic αPD-L1 induced complete tumor rejection in all of the mice tested across the three independent experiments conducted, significantly improving MTBVAC given as a monotherapy (figure 6D). In contrast, intravesical BCG or αPD-L1 alone did not provide any significant advantage compared with untreated mice, whereas BCG+αPDL1-induced efficacy resulted better than PBS or BCG alone, but substantially lower than the MTBVAC+αPDL1 combination (figure 6D). Altogether these results provide evidence that intravesical bacterial treatment of BC can be improved with systemic PD-L1 blockade.

DISCUSSION

Intravesical BCG, the first cancer immunotherapy ever approved by the FDA, has been the gold-standard therapy against NMIBC for more than four decades. Despite its success, there is a wide margin for improvement and the mechanism of action of this treatment remains incompletely understood, both from the point of view of the

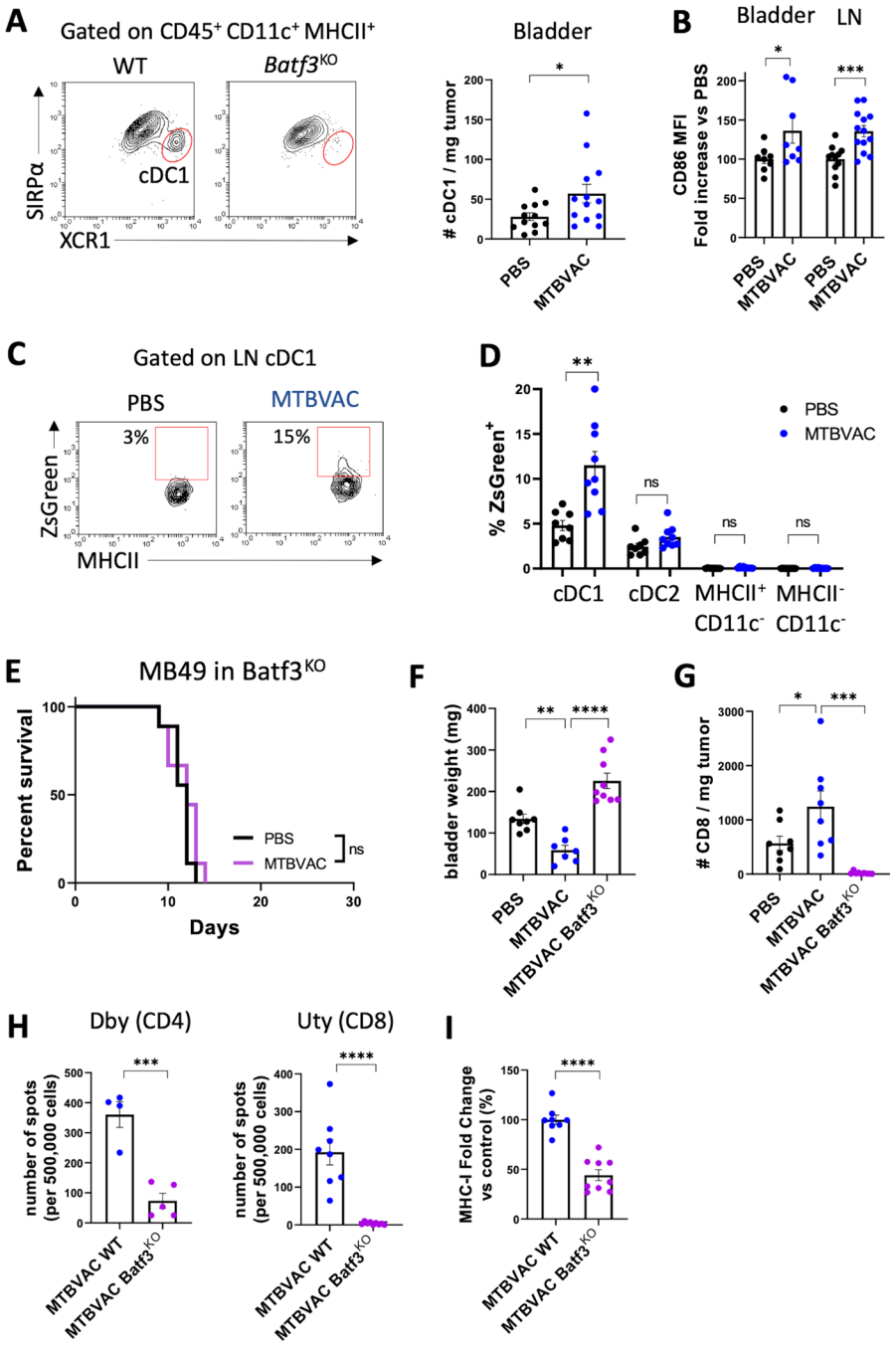

Figure 5 MTBVAC efficacy depends on type 1 conventional DCs. (A–C) MB49 cells were implanted intravesically and mice were treated with PBS or MTBVAC at days 3 and 10. At day 12, DCs were analyzed by flow cytometry in bladder and dLN single-cell suspensions. (A) Representative plot identifying XCR1^{+} cDC1s. Number of cDC1s per milligram of bladder tumor (n=12–13 mice per group, pooled from three independent experiments). (B) Normalized MFI of CD86 in bladder tumor-infiltrating and LN cDC1s (n=8 mice for bladder, pooled from two independent experiments and n=12–14 for LNs, pooled from three independent experiments). (C) Representative density plot of dLN cDC1s of mice inoculated with ZsGreen-expressing MB49 cells. (D) percentage of ZsGreen^{+} cells in distinct dLN cell compartments (n=8–9 mice per group, from two independent experiments). (E) Survival curve of Batf3^{KO} mice implanted orthotopically with MB49 cells and treated with PBS or MTBVAC at days 3, 10, and 17 (n=9 mice per group, two independent experiments). (F–I) WT or Batf3^{KO} mice were implanted with MB49 bladder tumors and received PBS or MTBVAC intravesically at days 3 and 10 (n=8–9 mice per group, from two independent experiments). (F) Bladder weights at day 12. (G) Number of infiltrating CD8^{+} T cells per milligram of tumor analyzed by flow cytometry in bladder single-cell suspensions. (H) IFN-γ-producing splenocytes stimulated with the Dby or Uty peptides. (I) Tumor cell MHC-I expression was measured by flow cytometry. Graph shows MHC-I expression fold change versus the control MTBVAC group (n=8–9 mice per group, from two independent experiments). Graphs represent mean±SEM. *P<0.05, **P<0.01, ***P<0.001, one-way analysis of variance with Bonferroni post-test (G,H), unpaired t-test (A,C,E,I,J), or log-rank test (F). DC, dendritic cell; dLN, draining lymph node; IFN-γ, interferon gamma; LN, lymph node; MFI, mean fluorescence of intensity; ns, not significant; WT, wild type.

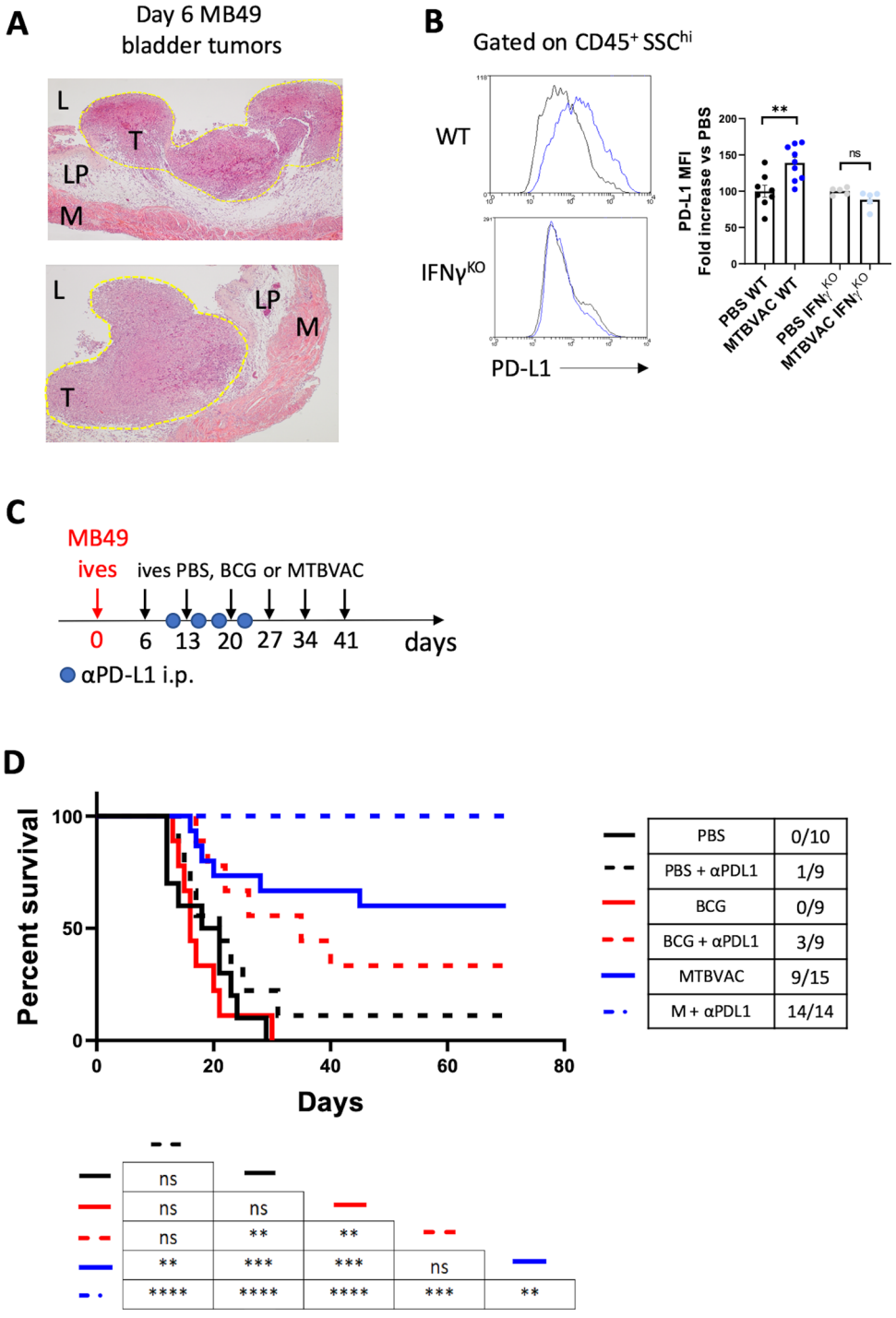

Figure 6 Improved bacterial immunotherapy rejects established bladder tumors. (A) Representative histology (H&E staining) of bladders 6 days after MB49 tumor cell inoculation. Tumor area is outlined in yellow. Letters denote the bladder lumen (L), lamina propia (LM), tumor (T) and muscle layer (M). (B) Representative histograms and quantification of PD-L1 MFI on the indicated cell type of mice bearing bladder tumors, treated intravesically on days 3 and 10 and analyzed on day 12. Graph shows PD-L1 expression fold change versus the control PBS of each mouse strain (n=5–9 mice per group, pooled from two independent experiments). (C) Schedule of intravesical treatments of mice bearing orthotopic MB49 bladder tumors with PBS or MTBVAC and intraperitoneal treatments with αPD-L1. (D) Survival of mice treated as in (C), (n=9–15 mice per group, pooled from three independent experiments). *P<0.05, **P<0.01, ***P<0.001, ****P<0.0001, log-rank test in (D), one-way analysis of variance with Bonferroni post-test in (B). IFN-γ, interferon gamma; MFI, mean fluorescence of intensity; ns, not significant; PD-L1, programmed cell death ligand 1; WT, wild type.

bacterial determinants of protection and the host immunological mechanisms. This treatment fails in up to 50% of patients, considering recurrence episodes and treatment withdrawals due to severe adverse events, which represent approximately 10% of BC cases.[27] Around 70% of the patients who suffer recurrence episodes following BCG

treatment undergo progression to T2 muscle-invasive disease, with radical cystectomy being the only therapeutic option in the clinical practice.[28] Moreover, BCG is not a unique strain but a diverse family of substrains with genetic heterogeneity. As a result, there are phenotypical differences among BCG substrains with respect to antigenicity and reactogenicity.[29] In fact, some studies have reported differences between the BCG strains Connaught and Tice in preventing BC recurrence and progression.[30 31] In this regard, MTBVAC represents a unique well-characterized vaccine strain which we have shown to induce a more potent antitumoral response in mice compared with BCG. Importantly, use of MTBVAC for BC treatment might translate in a reduction of bacterial dose and/or number of instillations, which could likely have an impact in the number of adverse effects produced currently by BCG.

It is well accepted that close contact between BCG and bladder epithelium is needed to achieve an optimal therapeutic effect.[32] Indeed, in vivo blocking of BCG bladder attachment in mouse models impairs treatment efficacy.[7] A lower antitumoral potency of heat-killed BCG has also been reported,[33] suggesting that bacteria do not bind passively to bladder epithelium, but that instead they employ active mechanisms to execute this process. Our results indicate that, compared with BCG, MTBVAC has an intrinsic better ability to colonize the bladder epithelium compared with BCG, in a process that seems to be mediated by ESAT6/CFP10 proteins. We have not characterized yet the molecular mechanisms by which ESAT6/CFP10 could be mediating bacterial attachment, but previous studies suggested a role for these proteins in *M. tuberculosis* attachment to lung epithelial cells through the extracellular matrix protein laminin.[20] Thus, we could speculate that mycobacteria-expressing ESAT6/CFP10 could bind to bladder epithelial cells through laminin in a similar manner as the described in the lung. Indeed, laminin is also present in bladder epithelial interstitium, with an augmented expression associated with bladder tumor development.[34]

Our studies demonstrate that MTBVAC treatment induces a tumor-specific response, and lack of therapeutic efficacy in Perf^{KO} and Rag1^{KO} mice suggested that CD8$^+$ T cells might be ultimately responsible for treatment success, a conclusion that is supported by the impaired treatment efficacy observed in mice challenged with *B2m*^{KO}-MB49 cells. Importantly, our rechallenge experiments confirm that therapy-induced tumor-specific immune memory is durable and functional against both localized and disseminated tumor cell rechallenge. A previous study reported that MHC-II neoantigens are required for efficient antitumor immunity, which implies a role for CD4$^+$ T cells.[35] In this regard, here we describe that bacterial immunotherapy enhances the CD4 tumor-specific response, and CD4$^+$ T-cell depletion completely abrogates the CD8 tumor-specific response and the vaccine therapeutic effect. More studies are needed to elucidate mechanisms by which CD4$^+$ T cells prime the CD8$^+$ response, but it is likely that the CD40/CD40L axis could have a role, since previous work identified that CD40 agonists eliminated bladder tumors by inducing a CTL response.[17] Moreover, CD4$^+$ T cell-secreted IFN-γ can upregulate MHC-I on tumor cells but could also have antiproliferative effects,[36] or enhance tumor cell sensitivity to cell death-inducing stimuli such as tumor necrosis factor (TNF) or Fas.[37]

Our work conducted in Batf3^{KO} mice indicates that cDC1s result crucial in the initiation of the tumor-specific CD4$^+$ and CD8$^+$ responses during MTBVAC therapy, as well as the infiltration of CD8$^+$ T cells into tumors. This DC subset is essential in cancer immune surveillance and is required for the response to other immunotherapies such as checkpoint blockade or αCD40.[17 38 39] Our data indicate that bacterial immunotherapy induces activation of cDC1, based on CD86 expression, and triggers a higher capacity of this cellular subset to acquire tumor-derived material and to carry it to the tumor dLNs, where antigen presentation and induction of tumor-specific responses are expected to occur. We could speculate a different hypothesis to explain how tumor cell material is initially generated and loaded into DCs. One is that bacteria themselves are inducing some degree of direct cytotoxicity over tumor cells. Indeed, our previous work described that MTBVAC was cytotoxic when incubated in vitro with different bladder tumor cell lines.[11] However, we must be cautious with this argument, since the conditions used in vitro, with dramatically higher multiplicities of infection and longer incubation time points, are very different from the settings applied here in vivo. Moreover, our present work indicates that the interaction between bacteria and non-immune cells (including tumor cells) in the bladder is very limited, and therefore it is unlikely that direct vaccine-induced toxicity over tumor cells has a major contribution in providing tumor-derived antigens to DCs. Conversely, we consider more plausible a main role of certain immune cells in this process, such as macrophages, neutrophils or natural killer (NK) cells, that may be activated by intravesical bacteria, kill a small portion of tumor cells and provide tumor-derived antigens to cDC1s, facilitating the initiation of adaptive immune responses. Our current data do not allow discernment of the exact mechanisms behind this process, and therefore more studies are needed to unravel the initial steps that occur after vaccine instillation.

Remarkably, we show that MTBVAC triggers rejection of fully established tumors in which BCG results are ineffective, which suggests that this improved bacterial therapy might be efficient against BCG-unresponsive tumors, for which few therapeutic options exist besides radical cystectomy. Interestingly, the antitumoral effect of MTBVAC was enhanced by blocking PD-L1, a therapeutic target that has been studied for BC with promising results.[40] Of note, our data demonstrated that MTBVAC induced PD-L1 upregulation in bladder immune cells. Several studies have correlated high levels of PD-L1 expression in tumor infiltrating immune cells with a better prognosis in different cancer types,[41] evidencing the existence

of a functional antitumor immune response. Indeed, it has been shown that IFN-γ produced by $CD8^+$ T cells upregulates the immunosuppressive mechanisms driven by indoleamine-2,3-dioxygenase and PD-L1 in the tumor microenvironment.[42] Our data suggest that the higher level of PD-L1 expression found on tumor-infiltrating immune cells is a consequence of enhanced IFN-γ production induced by bacterial treatment, and therefore it could be acting as surrogate marker of the vaccine-induced antitumoral response and sensitizing the tumor to checkpoint blockade immunotherapy.

Altogether, our data expand our understanding about how bacteria activate the immune system and induce efficient curative antitumor responses. In addition, they describe for the first time the proteins ESAT6 and CFP10 as determinants of intravesical bacterial immunotherapy efficacy against bladder tumors. These findings could be helpful in the future to develop more effective bacterial-based treatments against BC, either based on *M. tuberculosis* attenuated strains or improved versions of BCG, and provide a rationale for further evaluation of intravesical MTBVAC for NMIBC treatment.

Author affiliations
[1]Departamento de Microbiología, Pediatría, Radiología y Salud Pública, Universidad de Zaragoza/IIS Aragon, Zaragoza, Spain
[2]CIBERES, CIBERINFEC, Instituto de Salud Carlos III, Madrid, Spain
[3]Centre Hospitalier Universitaire Vaudois, Lausanne, Switzerland
[4]Hospital la Paz Institute for Health Research, IdiPAZ, Madrid, Spain
[5]Immunobiology Lab, Centro Nacional de Investigaciones Cardiovasculares Carlos III (CNIC), Madrid, Spain
[6]Grupo Zendal, Pontevedra, Spain
[7]Departamento de Inmunología y Oncología, CNB-CSIC, Madrid, Spain
[8]IIS Aragon/CIBA, Universidad de Zaragoza, Zaragoza, Spain

Twitter David Sancho @SanchoLab, Carlos Martín @CarlosMTBVAC and Nacho Aguilo @ElClubDarwin2

Acknowledgements We thank the Scientific and Technical Services from Instituto Aragonés de Ciencias de la Salud and Universidad de Zaragoza for their assistance.

Contributors Authors' contributions: EM, CM and NA designed the experiments. CM and NA supervised the study. EM, SU, AP and ABG performed the experiments. DN-H, CF, IM, EP, ER, JP and DS shared mouse lines or reagents. EM, DN-H, CF, IM, EP, ER, MV-G, JP, DS, CM and NA wrote the manuscript. NA is the guarantor of all the results shown in the study.

Funding This study was supported by Spanish Science and Innovation Ministry (RETOS COLABORACIÓN RTC-2017-6379-1 and RETOS INVESTIGACIÓN RTI2018-097625-B-I00); and 'Gobierno de Aragón-Fondo Europeo de Desarrollo Regional (FEDER) 2014-2020: Construyendo Europa Desde Aragón'. The funders had no role in study design, data collection and analysis, and decision to publish or preparation of the manuscript.

Competing interests SU, EP, ER, CM and NA are coinventors of the patent 'Compositions for use as a prophylactic agent to those at risk of infection of tuberculosis, or as secondary agents for treating infected tuberculosis patients' held by the University of Zaragoza and Biofabri. CM is inventor of the patent 'Tuberculosis vaccine' held by the University of Zaragoza. There are no other conflicts of interest.

Patient consent for publication Not applicable.

Ethics approval Experimental work was conducted in agreement with European and national directives for protection of experimental animals and experimental procedures were approved by the Ethics Committee for Animal Experiments of University of Zaragoza (PI46/18, PI33/15 PI50/14).

Provenance and peer review Not commissioned; externally peer reviewed.

Data availability statement Data are available upon reasonable request. All data relevant to the study are included in the article or uploaded as supplementary information. Availability of data and material: Data and materials available on request from the authors. Protected products included in the study are available by Material Transfer Agreement (MTA) procedure.

ORCID iDs
Eduardo Moreo http://orcid.org/0000-0002-0182-201X
Carlos del Fresno http://orcid.org/0000-0003-1771-7254
Julian Pardo http://orcid.org/0000-0003-0154-0730
David Sancho http://orcid.org/0000-0003-2890-3984
Carlos Martín http://orcid.org/0000-0003-2993-5478
Nacho Aguilo http://orcid.org/0000-0001-7897-9173

REFERENCES

1 Antoni S, Ferlay J, Soerjomataram I, *et al*. Bladder cancer incidence and mortality: a global overview and recent trends. *Eur Urol* 2017;71:96–108.
2 Morales A, Eidinger D, Bruce AW. Intracavitary Bacillus Calmette-Guerin in the treatment of superficial bladder tumors. *J Urol* 1976;116:180–2.
3 Gandhi NM, Morales A, Lamm DL. Bacillus Calmette-Guérin immunotherapy for genitourinary cancer. *BJU Int* 2013;112:288–97.
4 Decaestecker K, Oosterlinck W. Managing the adverse events of intravesical Bacillus Calmette–Guérin therapy. *Res Reports Urol* 2015;7:157–63.
5 Sylvester RJ. Bacillus Calmette-Guérin treatment of non-muscle invasive bladder cancer. *Int J Urol* 2011;18:113–20.
6 Pettenati C, Ingersoll MA. Mechanisms of BCG immunotherapy and its outlook for bladder cancer. *Nat Rev Urol* 2018;15:615–25.
7 Zhao W, Schorey JS, Bong-Mastek M, *et al*. Role of a Bacillus Calmette-Guérin fibronectin attachment protein in BCG-induced antitumor activity. *Int J Cancer* 2000;86:83–8.
8 Arbues A, Aguilo JI, Gonzalo-Asensio J, *et al*. Construction, characterization and preclinical evaluation of MTBVAC, the first live-attenuated M. tuberculosis-based vaccine to enter clinical trials. *Vaccine* 2013;31:4867–73.
9 Spertini F, Audran R, Chakour R, *et al*. Safety of human immunisation with a live-attenuated Mycobacterium tuberculosis vaccine: a randomised, double-blind, controlled phase I trial. *Lancet Respir Med* 2015;3:953–62.
10 Tameris M, Mearns H, Penn-Nicholson A, *et al*. Live-Attenuated Mycobacterium tuberculosis vaccine MTBVAC versus BCG in adults and neonates: a randomised controlled, double-blind dose-escalation trial. *Lancet Respir Med* 2019;7:757–70.
11 Alvarez-Arguedas S, Uranga S, Martín M, *et al*. Therapeutic efficacy of the live-attenuated Mycobacterium tuberculosis vaccine, MTBVAC, in a preclinical model of bladder cancer. *Transl Res* 2018;197:32–42.
12 Aguilo N, Gonzalo-Asensio J, Alvarez-Arguedas S, *et al*. Reactogenicity to major tuberculosis antigens absent in BCG is linked to improved protection against Mycobacterium tuberculosis. *Nat Commun* 2017;8:16085.
13 Domingos-Pereira S, Sathiyanadan K, La Rosa S, *et al*. Intravesical Ty21a vaccine promotes dendritic cells and T cell-mediated tumor regression in the MB49 bladder cancer model. *Cancer Immunol Res* 2019;7:621–9.
14 Ratliff TL, Palmer JO, McGarr JA, *et al*. Intravesical Bacillus Calmette-Guérin therapy for murine bladder tumors: initiation of the

response by fibronectin-mediated attachment of Bacillus Calmette-Guérin. *Cancer Res* 1987;47:1762–6.
15 Antonelli AC, Binyamin A, Hohl TM, *et al*. Bacterial immunotherapy for cancer induces CD4-dependent tumor-specific immunity through tumor-intrinsic interferon-γ signaling. *Proc Natl Acad Sci U S A* 2020;117:18627–37.
16 Biot C, Rentsch CA, Gsponer JR, *et al*. Preexisting BCG-specific T cells improve intravesical immunotherapy for bladder cancer. *Sci Transl Med* 2012;4:137ra72.
17 Garris CS, Wong JL, Ravetch JV, *et al*. Dendritic cell targeting with Fc-enhanced CD40 antibody agonists induces durable antitumor immunity in humanized mouse models of bladder cancer. *Sci Transl Med* 2021;13. doi:10.1126/scitranslmed.abd1346. [Epub ahead of print: 19 May 2021].
18 Gonzalo-Asensio J, Marinova D, Martin C, *et al*. MTBVAC: attenuating the human pathogen of tuberculosis (TB) toward a promising vaccine against the TB epidemic. *Front Immunol* 2017;8:1803.
19 Pym AS, Brodin P, Brosch R, *et al*. Loss of RD1 contributed to the attenuation of the live tuberculosis vaccines Mycobacterium bovis BCG and Mycobacterium microti. *Mol Microbiol* 2002;46:709–17.
20 Kinhikar AG, Verma I, Chandra D, *et al*. Potential role for ESAT6 in dissemination of M. tuberculosis via human lung epithelial cells. *Mol Microbiol* 2010;75:92–106.
21 Loskog A, Ninalga C, Hedlund T, *et al*. Optimization of the MB49 mouse bladder cancer model for adenoviral gene therapy. *Lab Anim* 2005;39:384–93.
22 Perez-Diez A, Joncker NT, Choi K, *et al*. CD4 cells can be more efficient at tumor rejection than CD8 cells. *Blood* 2007;109:5346–54.
23 Reyes RM, Deng Y, Zhang D, *et al*. CD122-directed interleukin-2 treatment mechanisms in bladder cancer differ from αPD-L1 and include tissue-selective γδ T cell activation. *J Immunother Cancer* 2021;9:e002051.
24 Philip M, Schietinger A. $CD8^+$ T cell differentiation and dysfunction in cancer. *Nat Rev Immunol* 2022;22:209–23.
25 Wculek SK, Cueto FJ, Mujal AM, *et al*. Dendritic cells in cancer immunology and immunotherapy. *Nat Rev Immunol* 2020;20:7–24.
26 Hildner K, Edelson BT, Purtha WE, *et al*. Batf3 deficiency reveals a critical role for CD8alpha+ dendritic cells in cytotoxic T cell immunity. *Science* 2008;322:1097–100.
27 Kamat AM, Flaig TW, Grossman HB, *et al*. Expert consensus document: consensus statement on best practice management regarding the use of intravesical immunotherapy with BCG for bladder cancer. *Nat Rev Urol* 2015;12:225–35.
28 Raj GV, Herr H, Serio AM, *et al*. Treatment paradigm shift may improve survival of patients with high risk superficial bladder cancer. *J Urol* 2007;177:1283–6.
29 Gan C, Mostafid H, Khan MS, *et al*. BCG immunotherapy for bladder cancer--the effects of substrain differences. *Nat Rev Urol* 2013;10:580–8.
30 Witjes JA, Dalbagni G, Karnes RJ, *et al*. The efficacy of BCG TICE and BCG Connaught in a cohort of 2,099 patients with T1G3 non-muscle-invasive bladder cancer. *Urol Oncol* 2016;34:484
31 Rentsch CA, Birkhäuser FD, Biot C, *et al*. Bacillus Calmette-Guérin strain differences have an impact on clinical outcome in bladder cancer immunotherapy. *Eur Urol* 2014;66:677–88.
32 Redelman-Sidi G, Glickman MS, Bochner BH. The mechanism of action of BCG therapy for bladder cancer--a current perspective. *Nat Rev Urol* 2014;11:153–62.
33 Kelley DR, Ratliff TL, Catalona WJ, *et al*. Intravesical Bacillus Calmette-Guerin therapy for superficial bladder cancer: effect of Bacillus Calmette-Guerin viability on treatment results. *J Urol* 1985;134:48–53.
34 Rousselle P, Scoazec JY. Laminin 332 in cancer: when the extracellular matrix turns signals from cell anchorage to cell movement. *Semin Cancer Biol* 2020;62:149–65.
35 Alspach E, Lussier DM, Miceli AP, *et al*. MHC-II neoantigens shape tumour immunity and response to immunotherapy. *Nature* 2019;574:696–701.
36 Alspach E, Lussier DM, Schreiber RD. Interferon γ and its important roles in promoting and inhibiting spontaneous and therapeutic cancer immunity. *Cold Spring Harb Perspect Biol* 2019;11. doi:10.1101/cshperspect.a028480. [Epub ahead of print: 01 Mar 2019].
37 Wang W, Green M, Choi JE, *et al*. $CD8^+$ T cells regulate tumour ferroptosis during cancer immunotherapy. *Nature* 2019;569:270–4.
38 Garris CS, Arlauckas SP, Kohler RH, *et al*. Successful anti-PD-1 cancer immunotherapy requires T Cell-Dendritic cell crosstalk involving the cytokines IFN-γ and IL-12. *Immunity* 2018;49:1148–61.
39 Sánchez-Paulete AR, Cueto FJ, Martínez-López M, *et al*. Cancer immunotherapy with immunomodulatory Anti-CD137 and anti-PD-1 monoclonal antibodies requires BATF3-Dependent dendritic cells. *Cancer Discov* 2016;6:71–9.
40 Zhou TC, Sankin AI, Porcelli SA, *et al*. A review of the PD-1/PD-L1 checkpoint in bladder cancer: from mediator of immune escape to target for treatment. *Urol Oncol* 2017;35:14–20.
41 Herbst RS, Soria J-C, Kowanetz M, *et al*. Predictive correlates of response to the anti-PD-L1 antibody MPDL3280A in cancer patients. *Nature* 2014;515:563–7.
42 Spranger S, Spaapen RM, Zha Y, *et al*. Up-Regulation of PD-L1, IDO, and T_{regs} in the Melanoma Tumor Microenvironment Is Driven by $CD8^+$ T Cells. *Sci Transl Med* 2013;5:1–21.

SUPPLEMENTARY MATERIAL

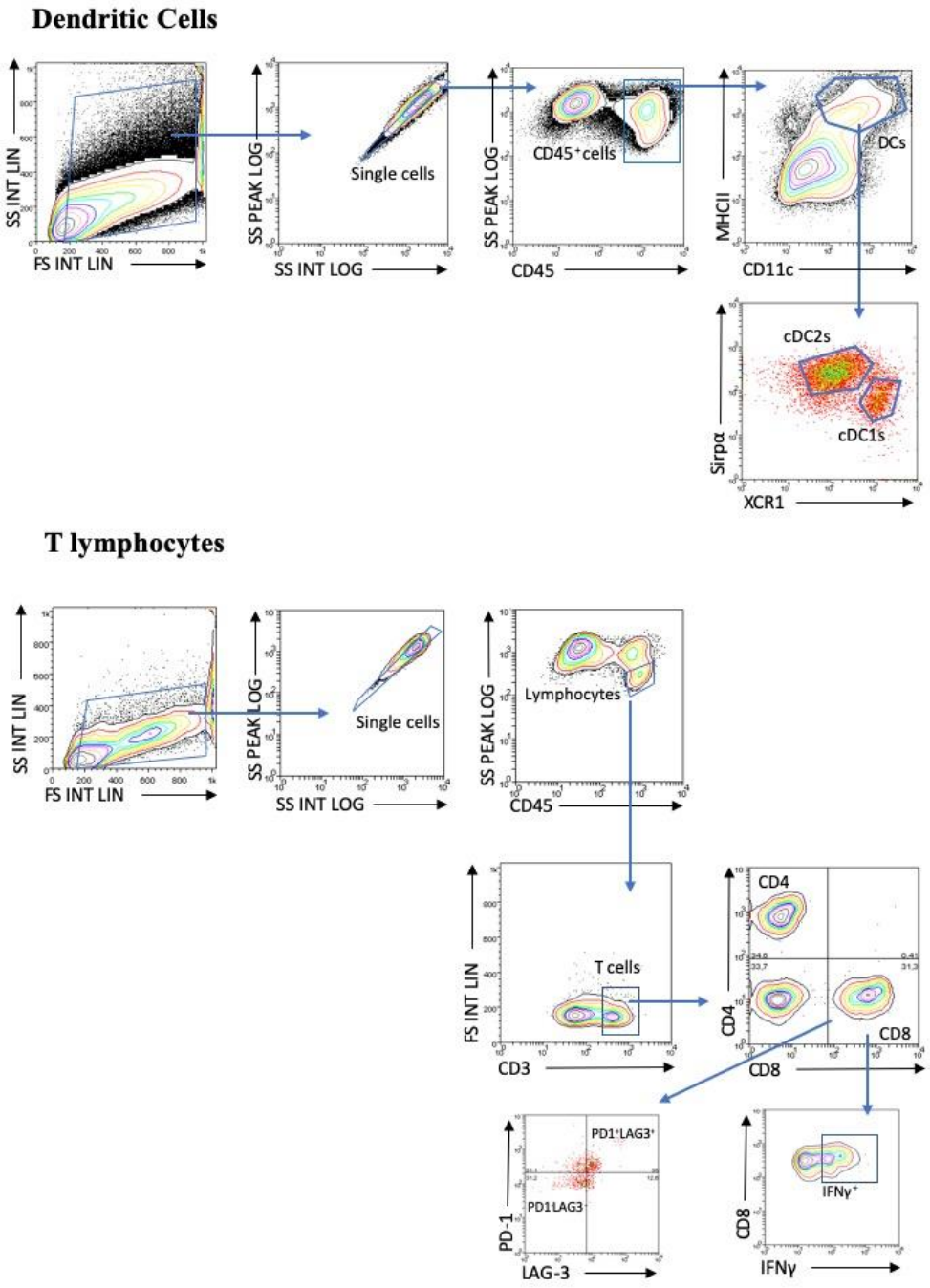

Fig S1. Bladder tumor gating strategy

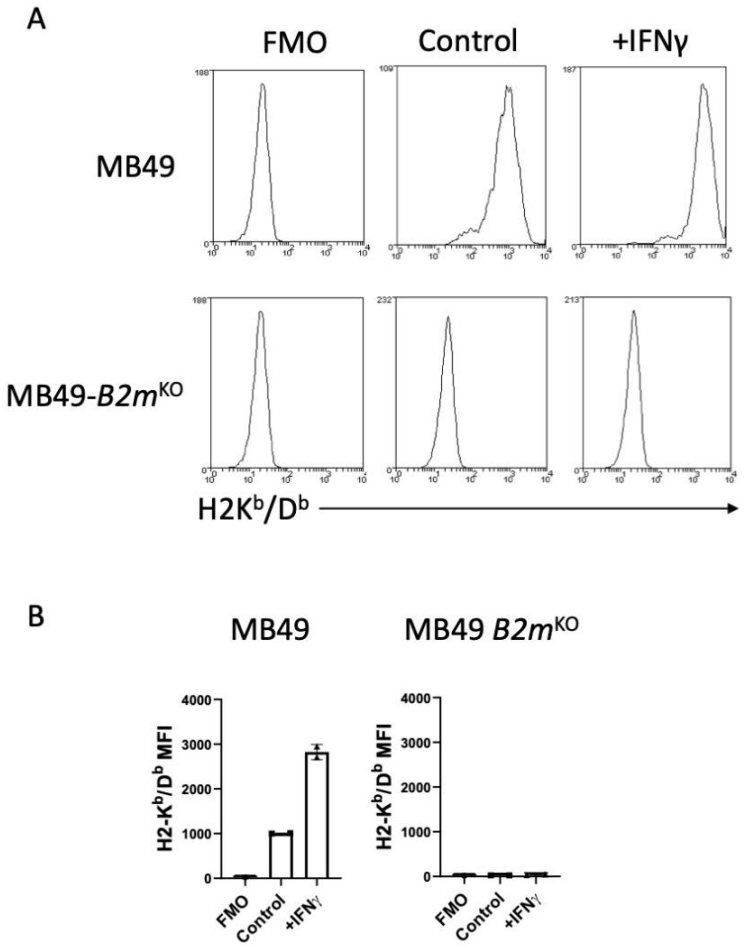

Fig S2. Characterization of MB49-B2mKO cells. (**A**) Representative histograms of H2Kb/Db expression on MB49 and MB49-B2mKO cells incubated for 24h with medium alone (control) or 50 ng ml-1 IFNγ. (**B**) Quantification of the mean fluorescence intensity (MFI) of H2Kb/Db in MB49 and MB49-B2mKO cells.

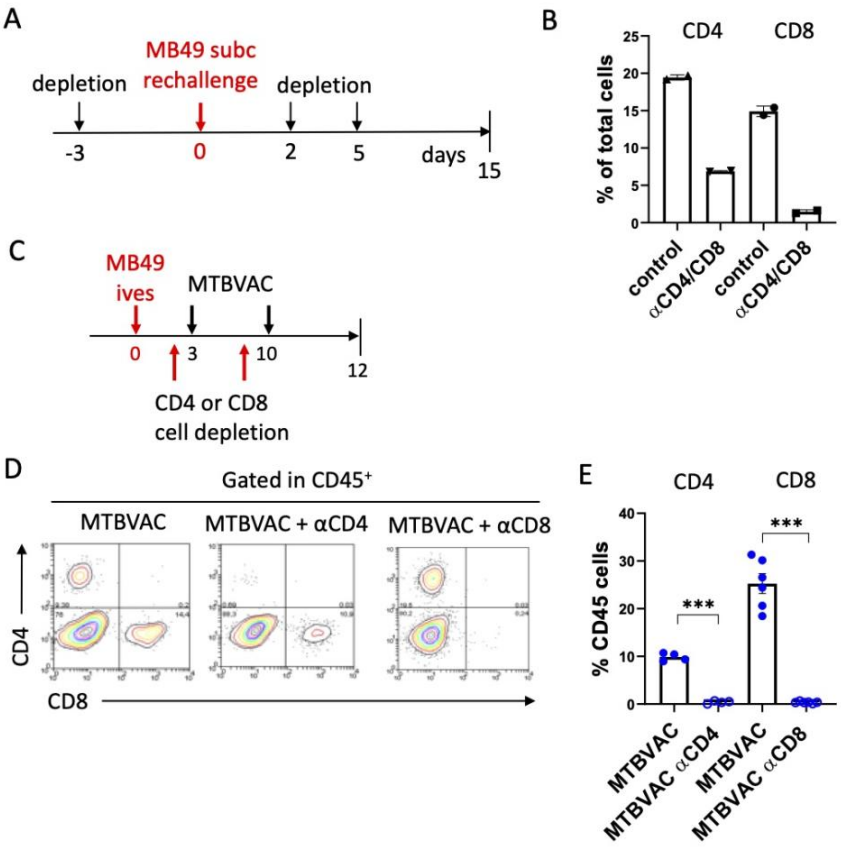

Fig S3. Antibody-based depletions. (A) Schedule of CD4 and CD8 depletion in the MB49 subcutaneous rechallenge experiments. When animals reached the predefined endpoint due to tumor burden, they were sacrificed and in two representative mice from each group, depletion efficiency was verified in the spleen. (B) Quantification of CD4 and CD8 T cells in the spleens of mice treated as in (A) n = 2 mice per group. (C) Schedule of CD4 or CD8 T cell depletion during intravesical MTBVAC therapy. (D) Flow cytometry density plots of T lymphocytes isolated from bladder tumors 12 days after MB49 cell implantation. Mice were treated intravesically with MTBVAC and were given αCD4 or αCD8 depleting antibodies twice. (E) Quantification of data from A, showing CD4 and CD8 T cell frequency in the CD45+ compartment. Graphs represent mean ± SEM. ***P<0.001, unpaired t test.